PREDICTING THE STRENGTH OF SAWN WOOD BY TRACHEID LASER SCATTERING

Mattias Brännström[a*], Janne Manninen[b], and Johan Oja[c]

An industrial laser light scattering scanner, designed to detect the spiral grain angle of logs by the light scattering along the grain, was used on two large samples of Norway spruce (*Picea abies* (var. Karst)) in various sawn dimensions (approximately 750 pieces). Additional measurements were made by other techniques, such as X-ray scanning, resonance frequency measurement, and various manual measurements. The strength properties of the boards were measured by destructive testing in four-point bending according to European standard. Multivariate methods (PLS) were used to model the relationship between the bending strength of the board (MOR) and the measurements. Based only on the output from the simple tracheid scattering equipment, a model for MOR achieved an R^2 exceeding 0.3. Combinations with average density or outer shape parameters from log scanning resulted in R^2 0.4 and 0.3 respectively, although these parameters alone only accounted for R^2 0.2. The results can be used to increase the understanding of strength in wood and in an improved industrial strength-grading process.

Keywords: Wood; Scanning; Strength grading; Log grading; Norway spruce; Spiral grain angle; Tracheid effect; Density; Laser; Multivariate models

*Contact information: a: (Luleå University of Technology and) Stora Enso Timber, SE-791 80 Falun, Sweden; b: Stora Enso Timber, P.O.Box 39, FI-06101 Porvoo, Finland; c: SP Technical research institute of Sweden, Skerìa 2, SE-931 77 Skellefteå, Sweden. *Corresponding author: mattias.brannstrom@storaenso.com*

INTRODUCTION

Wood fibers in softwoods form a spiral along the trunk, which is called spiral grain. The spiral grain of Norway spruce (*Picea abies* (var. Karst)) in northern Europe follows a pattern in which the helix has an approximately three-degree left-hand twist close to the pith. After about 80 years of growth, the angle becomes parallel to the stem, and after that slowly inclines to the right (Fig. 1) (Säll 2002). The change from left- to right-handed twist is the general pattern for trees in the northern hemisphere (Skatter and Kucera 1998). Large deviations from this pattern occur in Norway spruce, both in annual rings and between annual rings. Fertilization seems to have an effect according to some studies (Sarén et al. 2006), while others claim primarily that environmental factors have little impact and that heritage has much more influence on the spiral grain angle (Hannrup et al. 2004).

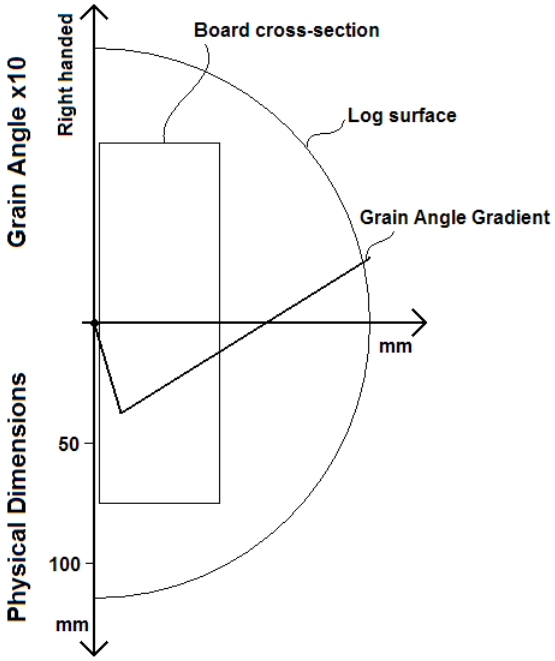

Fig. 1. Schematic description of the typical spiral grain angle development in Norway spruce, provided that the annual radial growth is about 1 mm. The grain angle is given relative to the cross-section of the board and the log top diameter for one of the samples in the study.

Some trees do not follow this pattern at all. Instead of turning from a left-handed to a right-handed helix, they tend to increase the left-handed angle with age. Boards from these specimens are also prone to twist more during drying. To be able to detect these logs and boards originating from them, automatic equipment has been developed (Nyström 2003). Recently, this equipment has also been made commercially available in different versions by The Swedish Testing and Research Institute, SP Trätek (Oja et al. 2006).

The equipment, called here a *tracheid effect scanner*, uses visible red laser illumination and a camera to detect the spiral grain angle on the surface of an object: log, block or board. The incident beam is scattered more easily in the direction of the grain (tracheids in softwoods) than perpendicular to it. The technique is well known as the tracheid effect and is widely used in various scanners. By employing the elliptical shape of the dot on the wooden surface, the grain angle in relation to the movement direction of the object can be calculated (Fig. 2). There are other parameters also derived from the image processing, such as eccentricity and area of the spot (Nyström 2003).

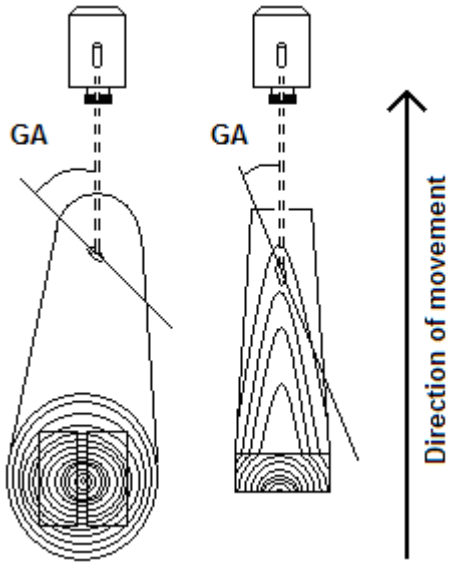

Fig. 2. A schematic description of grain angle measurement on logs and boards in longitudinal transport. This specimen with left-handed spiral grain represents an individual prone to distort during drying.

It is not only the grain angle in the longitudinal-tangential direction that can be determined by laser light scattering in wood. Several wood and fiber properties have been related to the scattering pattern, such as the angle in the longitudinal-radial direction, called "diving angle" (Simonaho and Silvennoinen 2004), density (Simonaho and Silvennoinen 2006), areas with high resin content, juvenile wood, compression wood and degradation of wood (Seltman 1992). It has been indicated that other properties, such as fiber length (Soest et al. 1993), pit density, and moisture content (Simonaho and Silvennoinen 2004; Simonaho et al. 2003), could also be revealed by, or at least influence, the pattern. Advanced models for light scattering in single wood fibers have also been created (Saarinen & Muinonen 2001).

It is a common view that the greater the grain angle, especially around local defects, the higher the reduction in strength, particularly tensile strength (Dinwoodie 2000). Galicki & Czech (2005) made a comparison of different models for tensile strength in pine and found that at high grain angle, tensile strength depends only on grain angle, while at low grain angle, tensile strength is controlled by a combination of grain angle and density. That study was done on small, clear and controlled samples. In larger sizes, telegraph poles of Douglas fir and Western Larch with a steep left-handed surface spiral grain (6°–7°) have about 50% reduced strength compared to right-hand twisted or straight-grained specimens (Lowery & Erickson 1967).

Various methods of machine strength grading are gaining popularity in the European woodworking industry, but visual strength grading is still in wide use. It has been shown that the grading accuracy of strength grading by Nordic visual rules (Anon. 1998) on Norway spruce is rather poor, $R^2 = 0.22$ for bending strength, compared to the best machines where R^2 ranges from 0.4 to 0.6. Among Nordic softwoods, the strength of spruce is generally more difficult to predict than that of pine (Hanhijärvi et al. 2005).

The results of previous research suggest that the grain angle should be a good variable for wood strength models, and recent development has enabled measurement of the variable with rugged and low cost equipment. Thus there is a need for an applied study of the technique in the strength grading field.

EXPERIMENTAL

This section describes the raw material used in the study, the industrial processing and the equipment used for measurements, the laboratory testing, image processing and analysis performed.

Wood Material

In this study, two samples of Norway spruce (*Picea abies* (var. Karst)) were used. The sampling was made timewise separated and by different criteria, due to other analysis than reported here, The first sample consisted of 120 logs with a top diameter of approximately 220 mm. The logs were selected randomly at a log yard of a sawmill in southern Finland.

The second sample consisted of a mixed sample of boards of various dimensions originating from Sweden, Finland, Russia and Estonia. Some boards in sample two came from the same sawmill as the logs in sample one. Dimensions and the number of boards in the 2nd sample can be found in Table 1. The boards were picked out at random, but only boards fulfilling at least the lowest quality demands were kept and planed. Butt, middle and top logs were represented, all with a top diameter in the range from 140 to 240 mm.

Table 1. The Number of Pieces Used in this Study from the 2nd Sample (after filtering), their Various Sizes and Origin.

Board Size [mm]			Origin [pcs]			
Thickness	Width	N	Sweden	Finland	Estonia	Russia
44	100	74	-	56	-	18
44	125	34	-	-	19	15
50	150	95	11	21	22	41
44	175	123	-	86	17	20
47	175	29	29	-	-	-
47	200	51	-	-	-	51
50	200	153	25	128	-	-
Total Number of pcs		559	65	291	58	145

Industrial Measurements, Devices and Processing

Table 2 lists the most important measurement equipment used in the study in the order of its use.

Table 2. An Overview of the Commercially Available Measurement Techniques used in the Study. All Equipment is of Industrial Standard.

Element in the Sawmilling Process	Manufacturer / Model	Method Applied
Log Sorting	Mikropuu 3D	3-D Log outer shape scanner
Log Sorting	SP / Snedfiber On-line	Tracheid effect scanner
Planing mill	Microtec / ViSCAN	Vibration frequency analyzer
Planing mill	Microtec / Golden Eye 702	Planar X-ray scanning
Planing mill	SP / Snedfiber On-line	Tracheid effect scanner

Industrial processing

The first sample was scanned as logs, for outer shape on bark, by a 3-D log outer-shape scanner, followed by scanning with the tracheid effect scanner after debarking. The logs were straight-sawn to retain two center boards (as in Fig. 2), nominal dimensions 50- x 150-mm. The boards were dried in a conventional progressive kiln and stabilized to about 16% moisture content during storage. After planing, the boards were analyzed with a vibration frequency analyzer and a planar X-ray scanner. Later, they were scanned again in another planing line with the tracheid effect scanner and finally destructive testing was made.

The second sample was also tested by the vibration frequency analyzer and the planar X-ray scanner (Anon. 2006b) after planing. After the destructive testing, the boards in the second sample were trimmed from the fracture, which left only shorter lengths, from 1.2 to 1.8 m. These shorter pieces were scanned with the tracheid effect scanner after some time in storage.

X-ray scanner and vibration frequency analyzer

The vibration frequency analyzer and the planar X-ray scanner are certified according European standard for strength grading (EN14081). The vibration frequency analyzer uses the well-known relation (equation 1) between first mode axial resonance frequency (f_{A-1}), length (L), density (ρ) and dynamic modulus of elasticity (E_{A-1}) (Ohlsson & Perstorper 1992). In this study, the relation was used without multiplying by the density value, being thus used only as an indication of the E_{A-1}. The planar X-ray scanner gives grayscale images of X-ray attenuation through the material. These images were not used for grading, but only to find knot information by image processing.

$$E_{A-1} = \rho \cdot (2 \cdot L \cdot f_{A-1})^2 \quad (1)$$

Tracheid effect scanning

The tracheid effect scanner consists of a laser, a camera, and a computer. The circular spot diode laser emits radiation at 660 nm with a power of 5 mW. A CCF 15 grayscale CMOS camera gathers information from the shape of the dot on the wood surface. The scanner gathers information along one line on the board with a sampling rate of 250 Hz. Internal algorithms is filtering the data to get registered measurements. To get a representative value, the grain angle directly over the pith (i. e. orthogonal to the pith direction) should be measured (Fig. 2). In practice, the measurement will vary slightly

from this position due to the irregular shape of the log; thus the varying pith position in the board.

For each board or log, several values are derived from the internal image analysis, such as mean eccentricity (*e*) of the ellipse according to equation 2, where *a* is the major axis and *b* is the minor axis. Further, the mean area of the ellipse (*A*), the mean, median and standard deviation of the global grain angle in relation to the direction of movement of the board (α_{mean}, α_{median} and α_{std} respectively) are derived. The grain angle is defined in this study as negative for left-handed spiral.

$$e = \frac{a - b}{b}, \quad (2)$$

All tracheid scanning was done along the centre of the tangential surfaces of the boards (Fig. 2). Data from the 2nd sample for boards with more than 30 registered measurements were kept for analysis. For the other boards, the variable values were assumed not to be safely representative of a whole board length and was thus omitted. Table 1 presents the material remaining after removing 39 observations.

Laboratory Testing and Analysis

This section describes the destructive testing, the image processing, the modeling and evaluation of the models.

Destructive testing

All boards were tested in four-point edgewise bending according to the European norm EN408 in two certified laboratories. The bending strength (Modulus of Rupture or MOR) and global Modulus of Elasticity (MOE) were determined.

After the destructive testing, the average ring width (ARW) in the first sample was measured manually at a position close to the fracture, from the pith diagonally to the farthest edge of the cross-section.

Density was measured on several occasions during the process. This was done as the average board density simply by dividing the weight by the volume, and as the clear wood density according to EN384.

Image processing

Some image processing was necessary to find the correlation between selected tracheid effect scanner variables and the number and size of knots at the centre of the board, i. e., at the measurement area for the tracheid effect scanner. The knot density sum and knot length in the center area of the board were found by a simple density threshold in the planar X-ray scanner images. The data analysis was performed in Matlab (Anon 2006a).

Statistical models and evaluation

Principal component analysis is suitable for analyzing data where noise and collinear variables are present. In this study, analysis was performed by Principal Component Analysis (PCA) and Partial Least Squares (PLS) in Simca-P, while normal

regression was analyzed in Excel (Lindgren 1994; Anon 2005; Anon 2003). For validation of the models, two data sets are usually used, the training set (TS) and the prediction set (PS). The prediction set was selected randomly distributed amongst the board dimensions in the second sample. A shortcut partly used in analysis of the first data set is to only use Q^2, the "goodness of prediction", without a separate prediction set (Wold 1978).

RESULTS AND DISCUSSION

Wood Strength Properties

The average wood strength properties varied between the samples (Table 3), which was expected, considering the differences between the two samples as to geographical coverage, origin and variation of the dimensions of the cross-section.

Table 3. Results from Destructive Testing. The Mean and Standard Deviations for Selected Strength and Wood Structural Properties of Both Samples. (Standard deviation within parentheses). ([1)] Average board density, [2)] small clear test piece cut close to fracture.)

Sample No	N	Bending Strength (N/mm²)		Modulus of Elasticity (N/mm²)		Density (kg/m³)		Annual Ring Width (mm)	
Sample 1	232	48.6	(11.6)	11020	(1570)	454 [1]	(31)	2.1	(0.7)
Sample 2	559	43.0	(13.4)	11558	(2138)	428 [2]	(44)	-	-

Board Strength Predictive Models

Models based only on the tracheid effect scanner variables explained more than one third of the variation in strength, and the stability of the models were good (R^2 and Q^2 were on the same level). By adding a density value, the predictive ability of the model increased, although density itself explained relatively little of the variation in strength (Table 4, Fig. 3, and Table 6). Models were made with the same variables on the first sample separately. For these models, no separate prediction set was made (Table 5).

Although there was some increase in R^2 (from 0.55 to 0.56 for both TS and PS) for a model including both an indication of the dynamic modulus of elasticity and the tracheid effect scanner variables, the Q^2 was reduced compared to the pure dynamic modulus model. This indicates that most of the wood properties measured by the laser are also measured by the resonance method, but not by density.

Simonaho and Silvennoinen (2006) found that the eccentricity of the ellipse (equation 2) increased with density. Although the measurement takes place at the surface, only about 50 mm from the pith, the density of the whole board is used as a reference. Spruce density varies greatly in the radial direction (Brännström 2004), which causes the value to be less representative. Instead, the mean eccentricity was most closely related to MOE (Table 4), which indicates that other wood or fiber properties than density alone are revealed by the measurement. One such example could be that compression wood, although of higher density, reduces the eccentricity of the ellipse (Seltman 1992; Nyström 1999).

Table 4. The correlation (r %) between Different Measures and Wood Properties. (The 1st sample. 'Center knot density sum' refers to the result of image processing of planar X-ray scanning images.)

(r sign) r² [%]	MOE	MOR	Average Density	ARW	Log Taper	Center Knot Density Sum
Mean eccentricity	54	43	34	-36	-3	-7
Mean grain angle	20	28	1	-17	5	-1
Std deviation grain angle	-49	-53	-13	43	-6	37
Mean laser spot area	31	29	5	-39	-18	-13
MOE	100	80	67	-59	2	2
MOR	80	100	46	-59	8	-6
Average density	67	46	100	-49	7	44
Annual ring width (ARW)	-59	-59	-49	100	-13	-11

Table 5. Strength Predictive PLS Models Based on the 1st Sample. Scaled and Centered Coefficients and Number of Principal Components in the Model (PC). (Since the coefficients are scaled and centered, the importance for the model can be estimated by the size of the coefficient.)

Equipment	Tracheid effect scanner	Tracheid effect scanner & Density	Tracheid effect scanner	3-D	Tracheid effect scanner & 3-D
State	Board	Board	Log	Log	Log
Constant	4.20	4.20	4.20	4.20	4.20
Mean angle	0.18	0.23	0.14		0.12
Std dev angle	-0.34	-0.34	-0.25		-0.21
Mean eccentricity	0.27	0.18	0.16		0.13
Mean area	0.19	0.12			
Manual density		0.33			
3D Volume				-0.11	-0.09
3D Sweep				0.17	0.15
3D Top taper				-0.26	-0.22
3D Butt taper				0.24	0.20
PC	1	2	1	1	1

Table 6. The Predictive Ability of the PLS Tracheid Effect Scanner Models for MOR Presented as the R^2 (goodness of fit) Q^2 (goodness of prediction) and RMSE (the root mean square error).

Equipment	Sample & Wood State	Data Set	R²	Q²	RMSE [N/mm²]
Tracheid effect scanner	1st board	Training set	0.40	0.38	9.0
	2nd board	Training set	0.34	0.32	11.5
	2nd board	Prediction set	0.34	-	10.3
Tracheid effect scanner & density	1st board	Training set	0.51	0.49	8.1
	2nd board	Training set	0.45	0.43	10.6
	2nd board	Prediction set	0.44	-	9.4
Tracheid effect scanner	1st log	Training set	0.15	0.13	10.7
3D outer shape	1st log	Training set	0.24	0.23	10.1
Tracheid effect scanner & 3D	1st log	Training set	0.34	0.31	9.5

Both R² and Q² were better for the model based on the 1st sample compared to the 2nd sample. The actual position of failure, and the surrounding wood, was not scanned for the 2nd sample while it was done for the 1st sample. The used variables were global for the whole board, consequently; Which part of the the board that is scanned should not have a great influence, but it cannot be stated for sure because some variation was lost by the method used. The lower precision for the 2nd sample can also come from the larger variation in board dimension and origin (Table 1).

Diving angle is a variable that should be greatly influenced by the sawing method. Boards from low-taper logs should have lower diving angle than those from higher-taper butt logs or top logs. Since this sample was straight-sawn, one can assume that the board surface consisted mainly of diving fibers. Thus, the low correlation between mean eccentricity of the ellipse and the shape of the log (Table 4) indicates that the diving angle has a small effect on the ellipse compared to other features influencing light scattering or simply that the variation in diving angle was too low due to the use of the same sawing technique for all boards.

With the destructive testing method used, the impact of knots along the centre line of the board should be minimal on strength. However, the knots along the centre might give an indication of knot properties on a global level for a board or log and thereby affect the correlation with strength. The knot density sum in the measured part of the board did explain a certain amount of the grain angle standard deviation value, as well as the strength. Sarén et al. (2006) found that the grain angle variation in the tangential-longitudinal plane is larger for wide annual rings. Hence, the degree of explanation added to the model by the standard deviation could come from the combined effect of knot variable measure and the annual ring width correlation.

The mean grain angle, with its negative average value (Table 7), is positively correlated to strength only vaguely (Table 4 and Table 5). This variable could increase in importance with a higher spatial resolution (several dots covering the whole width and thickness). According to the models, a large area and a high eccentricity are positive for strength. Density correlates weakly with eccentricity and not at all with spot area (Table 4).

Table 7. The Variation of Tracheid Effect Scanner Variables on the Different Scanning Occasions for the Samples. Median, Mean, and Standard Deviation for the Grain Angle (α_{mean}, α_{median} and α_{std}) and the Mean Eccentricity (*e*) and Area for the Scattered Ellipse on the Wood Surface (*A*). (The average values cannot be used for comparison due to lack of calibration between each run. Standard deviation within parentheses.)

Measured Surface and Sample Number	α_{median} [degrees]	α_{mean} [degrees]	α_{std} [degrees]	*E* [ ]	*A* [pixels]
Log, sample 1	-1.31 (2.16)	-1.37 (2.15)	1.81 (0.55)	0.99 (0.08)	553 (113)
Board, sample 1	0.31 (1.45)	0.17 (1.49)	2.66 (0.79)	1.09 (0.08)	335 (29)
Board, sample 2	-2.00 (1.50)	-2.12 (1.51)	2.33 (1.05)	1.43 (0.31)	179 (40)

The possible use of the tracheid effect scanner for strength grading purposes has been shown by the models evaluated (Table 5, Table 6, and Fig. 3). The results are not better than those from available grading machines, but even when used as stand-alone equipment, the tracheid effect scanner gives a higher R^2 than human visual grading (Hanhijärvi et al. 2005). Simple density measurement enhances the capabilities and the potential of the technique.

These results are limited to Norway spruce of uniform moisture content, unless moisture content correction can be established. More resinous wood might alter the response from the scattering measurement considerably (Seltman 1992).

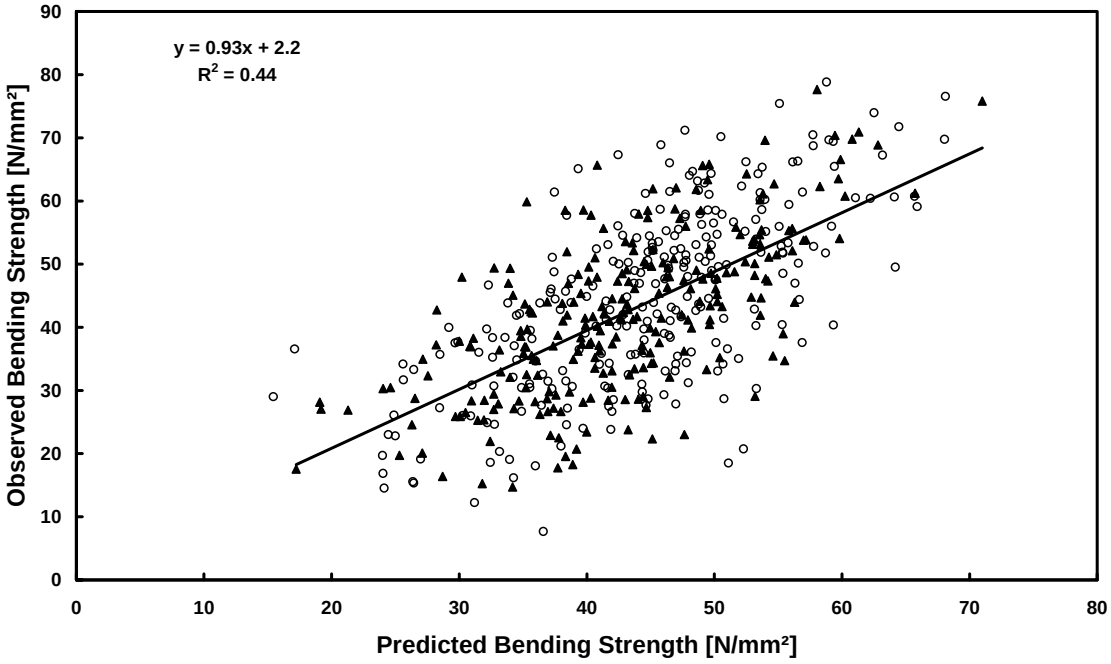

Fig. 3. Observed and Predicted MOR for the 2nd Sample. (Black triangles symbolize Prediction set and open circles symbolize Training set. Model based on tracheid effect scanner variables and global density of the boards. The model is presented in Table 5 and

Table 6. Regression line describes the Prediction set.)

Future research could focus on using more sensors, thereby covering a larger area of the board in the same way as several scanner manufacturers are doing today. The local grain angle could be utilized and the density and grain angle models of Galicki and Czech (2005) evaluated. It would also allow a better separation of the effect from different wood anatomy features on the diving angle, in such a way that it also could be used in the models. These results can serve as a base, a global strength estimation, in such an application.

Log strength grading

Log grading models were made for both the tracheid effect scanner and the 3-D frame as single machines and as a combination of them (Table 5 and Fig. 4). The degree of explanation of the models for bending strength was increased to $R^2 = 0.33$ and RMSE = 9.5 N/mm² (Table 6) by using combined techniques. In an earlier study, similar models were made by using log X-ray scanning information from the 1st sample (Brännström et al. 2007). The degree of explanation was better, $R^2 = 0.45$ and RMSE = 9.21 N/mm², but the cost and complexity of the equipment is much higher.

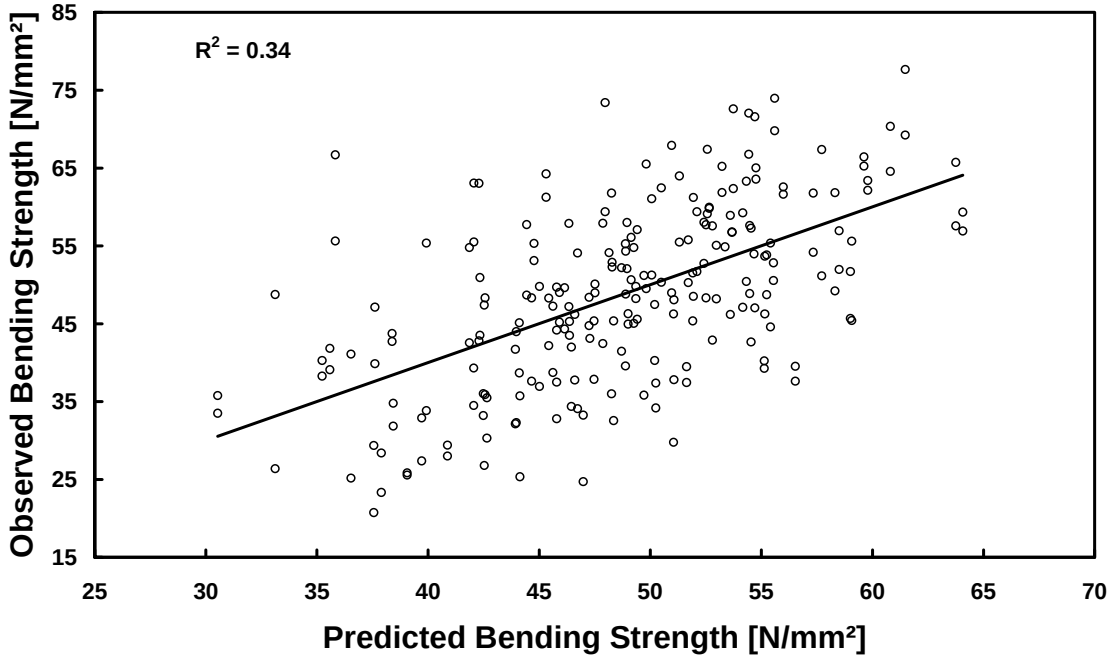

Fig. 4. Observed and Predicted MOR for the 1st Sample Training Set. Model Based on 3-D Outer Shape Measurements and Tracheid Effect Scanner Variables Measured on Logs. (The model is presented in Table 5 and Table 6.)

No stable models could be made for strength when using the log tracheid effect scanner variables only, although the relationship between median grain angle at the board surface and the median grain angle at the log surface in the first sample could be linearly described with r² 0.76 by equation 3.

$$GA_{BOARD} = 0.588 \cdot GA_{LOG} + 1.08 . \quad (3)$$

When measuring on rough surfaces, such as debarked logs or sawn boards, noise from the ripped surface is added to the measurement. Hence, the precision of each single grain angle measurement is not reliable, but the median values from two boards from the same log agree well, especially when considering that slightly different radial positions might have been measured (Fig. 5).

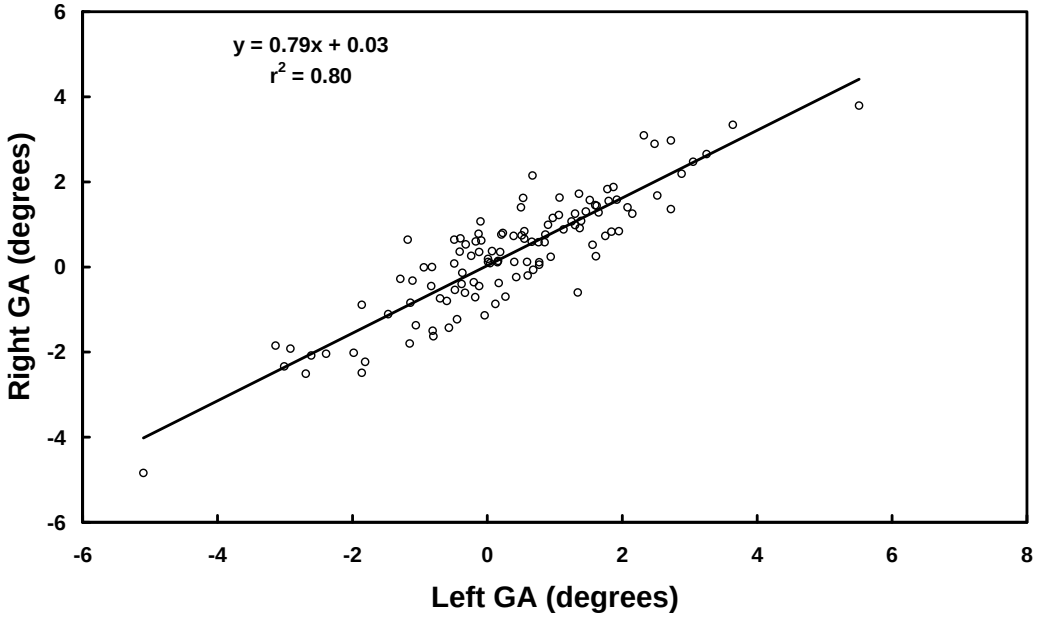

Fig. 5. A comparison of the median grain angle (α_{median}) from the left and right board (as they appeared in sawing) from each log. First sample.

When scanning the log surface, the variation within the annual rings is not available to the scanner. Thus, the standard deviation in grain angle now only refers to the low variation at the log surface. This value reflects more the quality of the debarking operations than the variation in wood properties (i. e., noise). Additionally, the moisture content has a large influence on the width of the ellipse on green material, while the length is less affected by moisture (Simonaho et al. 2003). Thus, homogeneous moisture content is a prerequisite for the successful use of the variable. The small contribution of the variable to the models might come from the influence of knots (Table 5) in a similar way as for the boards.

CONCLUSIONS

1. Tracheid effect scanning can be used for rough strength estimation on Norway spruce logs and sawn boards.
2. The grain angle standard deviation is more closely related to strength than the average grain angle when measured in a single line along the board length.
3. The scattering effects "Laser spot area" and "eccentricity of the spot" are related to wood properties of boards and can be used for grading purposes, provided that moisture content is uniform.

ACKNOWLEDGMENTS

These results have previously been briefly presented at the Workshop on nondestructive testing of wood products, Universidad del Biobio, Concepción, Chile, 11th–13th December 2006. This study was funded by the Skewood programme.

REFERENCES CITED

Anon. (1998). SS 23 01 20 *Träkonstruktioner – Konstruktionsvirke – Nordiskt T-virke– Visuella sorteringsklasser enligt INSTA 142.* (Swedish standard. Nordic visual strength grading rules for timber. In Swedish.) SIS Förlag AB 1998.

Anon. (2003). Microsoft Office Excel 2003 (11.6560.6568) SP2. [Computer software]. Microsoft corporation.

Anon. (2005). Simca-P (Version 11.0.0.0). [Computer software]. Sweden, Umeå: Umetrics AB.

Anon. (2006a). Matlab R2006a (v 7.2.0.232). [Computer Software]. Natick, MA: The Math Works.

Anon. (2006b). Microtec official homepage. Retrieved electronically 27 Oct. 2006 from [http://www.microtec.eu/].

Brännström, M. (2004). *Establishing a Model for the Dry Density of Heartwood of Norway Spruce by Parameters Industrially Measurable on Green Logs*. Masters thesis. Luleå University of Technology, no. 2005:207 CIV. ISSN: 1402-1617. Retrieved electronically 26 Oct. 2006 from [http://epubl.ltu.se/1402-1617/2005/207/index-en.html].

Brännström, M., Oja, J. , and Grönlund, A. (2007). "Predicting board strength by X-ray scanning of logs: The impact of different measurement concepts," *Scandinavian Journal of Forest Research* 22, 60–70.

Dinwoodie, J. M. (2000). *Timber: Its Nature and Behaviour* (2nd ed.). London: E & FN Spon.

EN384:2004:E. (2003). *Structural Timber - Determination of Characteristic Values of Mechanical Properties and Density*, European Committee for Standardization. Central Secretariat, Brussels.

EN408:2003:E. (2003). *Timber Structures - Structural Timber and Glued Laminated Timber - Determination of some Physical and Mechanical Properties*, European Committee for Standardization. Central Secretariat, Brussels.

EN14081-4:2005/A3:2007(E). (2007) *Timber Structures – Strength Graded Structural Timber with Rectangular Cross Section – Part 4: Machine Grading – Grading Machine Settings for Machine Controlled Systems.* European Committee for standardization. Central Secretariat, Brussels.

Galicki, J., and Czech, M. (2005). "Tensile strength of softwood in LR orthotropy plane," *Mechanics of Materials* 37: 677–686.

Hanhijärvi, A., Ranta-Maunus, A., and Turk, G. (2005). *Potential of Strength Grading of Timber with Combined Measurement Techniques.* Report of the Combigrade-project

–phase 1 (VTT Publications 568). Retrieved 31 Oct. 2005 from http://www.vtt.fi/inf/pdf.

Hannrup, B., Cahalan, C., Chantre, G., Grabner, M., Karlsson, B., Le Bayon, I., Jones, G. L., Muller, U., Pereria, H., Rodrigues, J. C., Rosner, S., Rozenberg, P., Wilhelmsson, L., and Wimmer, R. (2004). "Genetic parameters of growth and wood quality traits in *Picea abies*," *Scandinavian Journal of Forest Research* 19 (1), 14–29.

Lindgren, F. 1994. *Third Generation PLS: Some Elements and Application*. PhD thesis, Umeå University (Department of organic chemistry, Research group for chemometrics), Sweden.

Lowery, D. P., and Erickson, E. C. O. (1967). *The Effect of Spiral Grain in Pole Twist and Bending Strength*. U.S. Forest Service Research Paper, INT-35.

Nyström, J., and Hagman, O. (1999). "Methods for detection of compression wood in green and dry conditions," In: *Proceedings from Polarization and Color Techniques in Industrial Inspection*. Munich, Germany, June 14–18, 1999.

Nyström, J. (2003). "Automatic measurement of fiber orientation in softwoods by using the tracheid effect," *Computers and Electronics in Agriculture* 41 (1), 91–99.

Ohlsson, S., and Perstorper, M. (1992). "Elastic wood properties from dynamic tests and computer modeling," *Journal of Structural Engineering* 118 (10): 2677–2690.

Oja, J., Grundberg, S., Berg, P., and Fjellström, P.-A. (2006). *Equipment for Measuring Fibre Angle and Heartwood Content in Sawn Wood during Transverse Feed in the Green Sorting* (In Swedish with English abstract). SP Swedish National testing and research institute. SP Report 2006:16. ISBN 91-8533-01-7.

Sarén, M. P., Serimaa, R., and Tolonen, Y. (2006). "Determination of fiber orientation in Norway spruce using X-ray diffraction and laser scattering," *Holz als Roh- und Werkstoff* 64, 183–188.

Saarinen, K., and Muinonen, K. (2001). "Light scattering by wood fibers," *Applied Optics* 40 (28), 5064–5077.

Seltman, J. (1992). "Indication of slope-of-grain and biodegradation in wood with electromagnetic waves," In: Lindgren, O. (Ed.), *1st International Seminar on Scanning Technology and Image processing on Wood*. Luleå University of Technology, Skellefteå, Sweden.

Simonaho, S.-P., Tolonen, Y., Rouvinen, J., and Silvennoinen, R. (2003). "Laser light scattering from wood samples soaked in water or in benzyl benzoate," *Optik* 114 (10), 445–448.

Simonaho, S.-P., and Silvennoinen, R. (2004). "Light diffraction from wood tissue," *Optical Review* 11 (5), 308–311.

Simonaho, S.-P., Palviainen, J., Tolonen, Y., and Silvennoinen, R. (2004). "Determination of wood grain direction from laser light scattering pattern," *Optics and Lasers in Engineering* 41, 95–103.

Simonaho, S.-P., and Silvennoinen, R. (2006). "Sensing of wood density by laser light scattering pattern and diffractive optical element based sensor," *Journal of Optical Technology* 73 (3), 170–174.

Skatter, S., and Kucera, B. (1998). "The cause of the prevalent direction of the spiral grain pattern in conifers," *Trees* 12, 265–273.

Soest, J., Matthews, P., and Wilson, B. (1993). "A simple optical scanner for grain defects," In: *Proceedings from the 5th International Conference on Scanning Technology & Process Control for the Wood Products Industry*. Atlanta, GA.

Säll, H. (2002). *Spiral grain in Norway spruce.* (Doctoral thesis). Acta Wexionensia No22/2002. Växjö, Växjö University Press. ISBN 91-7636-356-2.

Wold, S. (1978). "Cross-validatory estimation of the number of components in factor and principal components models," *Technometrics* 20, 397–405.

Article submitted: Jan. 24, 2008; Peer review completed: Feb. 23, 2008; Revised article received and accepted: March 18, 2008; Published March 26, 2008.